Shields, G.A., and Mills, B.J.W., 2020, Evaporite weathering and deposition as a long-term climate forcing mechanism: Geology, v. 49, https://doi.org/10.1130/G48146.1

Supplementary Material

Supplementary information 1: Carbon-alkalinity-calcium deep time box model

This model is designed to track the transfer of atmospheric and marine carbon over geological time, while including explicit representation of the calcium and alkalinity cycles and how they control carbonate deposition. The biogeochemical system is taken largely from the work of Walker and Kasting (1992), with some additions from Rampino and Caldeira (2005), Payne and Kump (2007) and Clarkson et al. (2015), with the underlying hydrological model from Sarmiento and Toggweiler (1984).

1. Model structure

The model we use is slightly modified from the model of Dal Corso et al. (2020). For this work we remove the Hg cycle and add a simple Ca cycle. All other model processes remain identical. For convenience we reproduce the model derivation here. The model has three ocean boxes: surface (s), high-latitude (h) and deep (d). As in Sarmiento and Toggweiler (1984) the surface box is 100 m deep and occupies 85% of the ocean surface, whereas the high-latitude box is 250 m deep and represents 15% of the ocean surface. Each ocean box includes the same biogeochemical species, and a thermohaline circulation mixes the boxes in the order s, h, d. The upper boxes exchange with the atmosphere, which is a single box. As well as transfer fluxes between ocean and atmosphere boxes, biogeochemical fluxes of weathering, degassing and burial operate between the surface system and crust. The model schematic is shown in figure 1 below.

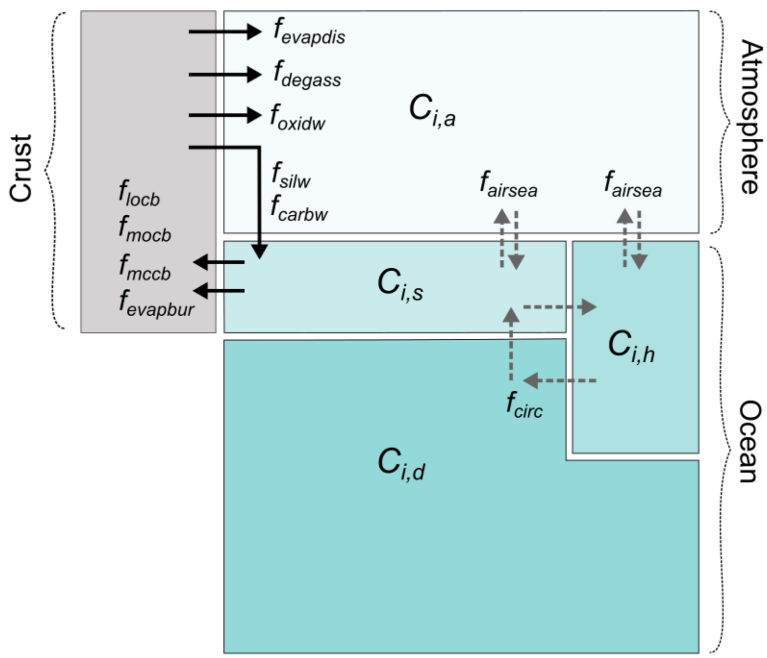

Figure S1. Model schematic. *Concentrations of modelled species are tracked in boxes representing the atmosphere (a), surface ocean (s), high-latitude ocean (h) and deep ocean (d). Exchange between boxes via air-sea exchange and circulation and mixing are shown as dashed arrows. Biogeochemical fluxes between the hydrosphere and continents/sediments are shown as solid arrows. See text for full details of fluxes.*

2. Model species

Model species are shown in table S1 below.

Description	Name	Exists in	Size at present
Surface ocean water	W_s	Surface Ocean	3.07×10^{16} m^3
High-latitude water	W_h	High Latitude	1.35×10^{16} m^3
Deep water	W_d	Deep ocean	1.35×10^{18} m^3
Atmospheric CO_2	CO_{2_a}	Atmosphere	5×10^{16} mol C
Surface ocean DIC	DIC_s	Surface Ocean	6×10^{16} mol C *
High-latitude DIC	DIC_h	High Latitude	3×10^{16} mol C *
Deep ocean DIC	DIC_d	Deep ocean	3×10^{18} mol C*
Surface ocean alkalinity	ALK_s	Surface Ocean	6×10^{16} mol $CaCO_3$ equiv. *
High-latitude alkalinity	ALK_h	High Latitude	3×10^{16} mol $CaCO_3$ equiv. *
Deep ocean alkalinity	ALK_d	Deep ocean	3×10^{18} mol $CaCO_3$ equiv. *
Surface ocean calcium	CAL_s	Surface Ocean	3.1×10^{17} mol Ca

High-latitude calcium	CAL_h	High Latitude	1.4×10^{17} mol Ca
Deep ocean calcium	CAL_d	Deep ocean	1.4×10^{19} mol Ca

*starting values chosen close to equilibrium values, model equilibrates to DIC ≈ 2 mM and ALK≈ 2.2 mM, roughly approximate to the modern ocean. Other values follow Sarmiento and Toggweiler (1984) and Lenton et al., (2018).

3. Model fluxes

Model fluxes, with equations and present values are shown in table S2 below. Transfer fluxes follow a simple concentration relationship, air sea exchange follows Walker and Kasting (1992), carbonate burial (net accumulation) follows Rampino and Caldeira (2005) and all other fluxes are chosen from recent carbon cycle models (Lenton et al., 2018). Degassing shown in figure S1 sums carbonate and organic carbon degassing.

Description	Name	Equation	Size at present
Transfer fluxes	$tran_{ij}$	$C_i f_{circ}$	Multiple
Air sea exchanges	f_{airsea_j}	$A_j M_{atm}(\frac{pCO_{2_a} - pCO_{2_j}}{\tau_{oa}})$	Multiple
Silicate weathering	f_{silw}	$k_{basw} f_{T_{bas}} + k_{granw} f_{T_{gran}}$	8×10^{12} mol C yr^{-1}
Carbonate weathering	f_{carbw}	$k_{carbw} f_{Tcarb}$	8×10^{12} mol C yr^{-1}
Oxidative weathering	f_{oxidw}	$k_{oxidw}(RO_2)^{0.5}$	7.75×10^{12} mol C yr^{-1}
Carbonate degassing	f_{ccdeg}	k_{ccdeg}	8×10^{12} mol C yr^{-1}
Organic carbon degassing	f_{ocdeg}	k_{ocdeg}	1.25×10^{12} mol C yr^{-1}
Marine carbonate burial	f_{mccb}	$k_{mccb} \frac{(\Omega - 1)^{1.7}}{\Omega_0}$	16×10^{12} mol C yr^{-1}
Marine organic C burial	f_{mocb}	k_{mocb}	4.5×10^{12} mol C yr^{-1}
Land organic C burial	f_{locb}	k_{locb}	4.5×10^{12} mol C yr^{-1}
Evaporite dissolution	$f_{evapdis}$	$k_{evapdis}$	Varied in experiments
Evaporite deposition	$f_{evapdep}$	$k_{evapdep}$	Varied in experiments

4. Non-flux calculations

Atmospheric CO_2 volume ratio:

$$CO_2ppm = 280\frac{CO_{2_a}}{CO_{2_{a_0}}}$$

where CO_{2_a} is atmospheric CO_2 in moles, and $CO_{2_{a_0}}$ is this value at present day.

Global average surface temperature:

$$GAST = 288 + k_{clim}\left(\frac{\log(\frac{CO_2ppm}{280})}{\log(2)}\right)$$

where t_{clim} is climate sensitivity to doubling CO_2. Low-latitude surface temperature (T_s) is assumed to scale by $\frac{2}{3}$ times global temperature change, and both high-latitude (T_h) and deep ocean (T_d) temperature are assumed to follow global temperature change.

Carbonate speciation:

Effective equilibrium constants are calculated following Walker and Kasting (1992), after Broecker and Peng (1982). These consider only temperature dependencies, omitting those on pressure and salinity.

$$K_{carb} = 5.75\times10^{-4} + 6\times10^{-6}(T_j - 278)$$

$$K_{CO_2} = 0.035 + 0.0019(T_j - 278)\ \text{PAL m}^3\ \text{mol}^{-1}$$

Dissolved carbon species are then calculated following Walker and Kasting (1992):

$$[HCO_3^-]_j = DIC_j - \frac{\sqrt{DIC_j^2 - ALK_j\left(2DIC_j - ALK_j\right)(1 - 4K_{carb})}}{1 - 4K_{carb}}$$

$$[CO_3^{2-}]_j = \frac{ALK_j - [HCO_3^-]_j}{2}$$

$$pCO_{2_j} = \frac{K_{CO_2}[HCO_3^-]^2}{[CO_3^{2-}]}$$

Calcium carbonate saturation state:

$$\Omega_j = \frac{[Ca]_j[CO_3^{2-}]_j}{K_{sp}}$$

where Ω_j is the $CaCO_3$ saturation state in box j and K_{sp} is the solubility product. [Ca] and $[CO_3^{2-}]$ are concentrations.

Terrestrial chemical weathering

Temperature dependence of basalt and granite weathering:

$$f_{T_{bas}} = e^{0.0608(GAST-288)}(1+0.038(GAST-288))^{0.65}$$

$$f_{T_{gran}} = e^{0.0724(GAST-288)}(1+0.038(GAST-288))^{0.65}$$

Temperature dependence of carbonate weathering:

$$f_{T_{carb}} = 1 + 0.087(GAST - 288)$$

Weathering constants:

$$k_{basw} = 2.4 \times 10^{12} \text{ mol yr}^{-1}$$

$$k_{granw} = 5.6 \times 10^{12} \text{ mol yr}^{-1}$$

5. Fixed parameters

Fixed parameters are shown in table S3.

Description	Name	Size at present
Thermohaline speed	f_{circ}	20 Sv
Relative area of low-latitude surface ocean	A_s	0.85
Relative area of high-latitude surface ocean	A_h	0.15
Present day moles of atmospheric CO_2	M_{atm}	5×10^{16} mol C
Timescale parameter for gas exchange	τ_{oa}	10 years
Long-term climate sensitivity	k_{clim}	5 K
Calcium carbonate solubility product	K_{sp}	0.8 $\text{mmol}^2\ \text{kg}^{-2}$ *
Present day $CaCO_3$ saturation state	Ω_0	3

*chosen within ocean range (0.43-1.15) (Zeebe and Wolf-Gladrow, 2001) to achieve reasonable DIC and ALK at present. Other parameters follow Walker and Kasting (1992), Sarmiento and Toggweiler (1984), Clarkson et al. (2015). Long-term climate sensitivity (Lunt et al., 2009) is larger than equilibrium climate sensitivity (ECS), and appears to be around 5K during the Phanerozoic (Mills et al., 2019).

6. Differential equations

The following equations track the 11 non-water species from table 1.

Atmospheric CO_2:

$$\frac{d(CO_{2_a})}{dt} = -f_{airsea_s} - f_{airsea_h} + f_{ccdeg} + f_{ocdeg} + f_{oxidw} - f_{locb} - f_{carbw} - 2f_{silw}$$

Low-latitude surface ocean DIC

$$\frac{d(DIC_s)}{dt} = f_{airsea_s} + tran_{DIC_{ds}} - tran_{DIC_{sh}} + 2f_{carbw} + 2f_{silw} - f_{mccb} - f_{mocb}$$

High-latitude surface ocean DIC

$$\frac{d(DIC_h)}{dt} = f_{airsea_h} + tran_{DIC_{sh}} - tran_{DIC_{hd}}$$

Deep ocean DIC

$$\frac{d(DIC_d)}{dt} = tran_{DIC_{hd}} - tran_{DIC_{ds}}$$

Low-latitude surface ocean alkalinity

$$\frac{d(ALK_s)}{dt} = tran_{ALK_{ds}} - tran_{ALK_{sh}} + 2f_{carbw} + 2f_{silw} - 2f_{mccb}$$

High-latitude surface ocean alkalinity

$$\frac{d(ALK_h)}{dt} = tran_{ALK_{sh}} - tran_{ALK_{hd}}$$

Deep ocean alkalinity

$$\frac{d(ALK_d)}{dt} = tran_{ALK_{hd}} - tran_{ALK_{ds}}$$

Low-latitude surface ocean Ca

$$\frac{d(ALK_s)}{dt} = tran_{CAL_{ds}} - tran_{CAL_{sh}} + f_{carbw} + f_{silw} - f_{mccb} + f_{evapdis} - f_{evapdep}$$

High-latitude surface ocean Ca

$$\frac{d(ALK_h)}{dt} = tran_{CAL_{sh}} - tran_{CAL_{hd}}$$

Deep ocean Ca

$$\frac{d(ALK_d)}{dt} = tran_{CAL_{hd}} - tran_{CAL_{ds}}$$

7. Model solution

The model is solved in MATLAB using the ODE15s variable-order method for stiff systems. Code is available on request to BJWM.

8. References

Clarkson, M. O. et al. Ocean acidification and the Permo-Triassic mass extinction. *Science* **348,** 229-232 (2015).

Dal Corso, J. et al. Permo–Triassic boundary carbon and mercury cycling linked to terrestrial ecosystem collapse. *Nature Communications* **11,** 2962 (2020).

Lenton, T.M., Daines, S.J., and Mills, B.J.W., 2018, COPSE reloaded: An improved model of biogeochemical cycling over Phanerozoic time: Earth-Science Reviews, v. 178, p. 1–28, doi:10.1016/j.earscirev.2017.12.004.

Lunt, D. J. et al. Earth system sensitivity inferred from Pliocene modelling and data. Nature Geoscience 3, 60-64 (2009).

Mills, B. J. W. et al. Modelling the long-term carbon cycle, atmospheric CO2, and Earth surface temperature from late Neoproterozoic to present day. Gondwana Research 67, 172-186 (2019).

Payne, J. & Kump, L. Evidence for recurrent Early Triassic massive volcanism from quantitative interpretation of carbon isotope fluctuations. *Earth and Planetary Science Letters* **256,** 264-277 (2007).

Rampino, M. R. & Caldeira, K. Major perturbation of ocean chemistry and a 'Strangelove Ocean' after the end-Permian mass extinction. *Terra Nova* **17,** 554-559 (2005).

Sarmiento, J. L. & Toggweiler, J. R. A new model for the role of the oceans in determining atmospheric pCO_2. *Nature* **308,** 621-624 (1984).

Walker, J.G.C. & Kasting, J.F. Effects of fuel and forest conservation on future levels of atmospheric carbon dioxide. *Paleogeography, Paleoclimatology, Paleoecology* **97,** 151-189 (1992).

Zeebe, R. R. & Wolf-Gladrow, D. CO_2 in seawater: equilibrium, kinetics, isotopes. Elseveir (2001).